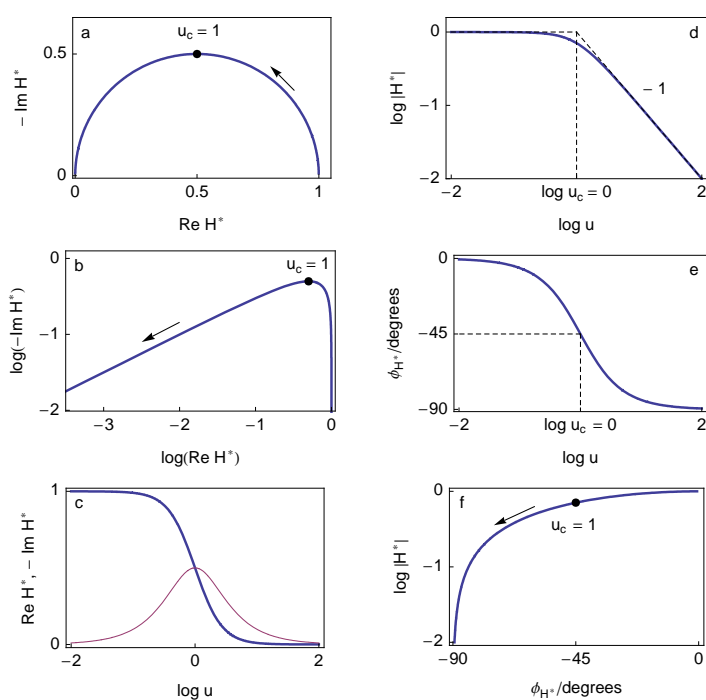


Handbook of Electrochemical Impedance Spectroscopy



TRANSFER FUNCTIONS

ER@SE/LEPMI
J.-P. Diard, B. Le Gorrec, C. Montella

Hosted by Bio-Logic @ www.bio-logic.info



January 4, 2009

Contents

1	Graphs of transfer functions	5
1.1	Introduction [1]	5
1.2	Nyquist diagram	6
1.2.1	Nyquist diagram used by electricians	6
1.2.2	Nyquist diagram used by electrochemists	6
1.3	Bode diagram	6
1.3.1	Bode diagram used by electricians	6
1.3.2	Bode diagram used by electrochemists	6
1.4	Black diagram	6
1.4.1	Black diagram used by electrician	6
1.4.2	Black diagram used by electrochemists	6
1.5	Miscellaneous	7
2	First-order transfer functions	9
2.1	First-order transfer function [2, 7]	9
2.1.1	First-order transfer function	9
2.1.2	Dimensionless first-order transfer function	9
2.2	Generalized first-order transfer functions	11
2.2.1	High-pass first-order transfer function	11
2.2.2	Dimensionless high-pass first-order transfer function	11
2.2.3	Generalized first-order transfer function	11
2.2.4	Dimensionless generalized first-order transfer function	11
3	Second-order transfer functions	15
3.1	Introduction	15
3.1.1	Canonical form	15
3.1.2	Reduced form	15
3.1.3	Second-order transfer function with real poles	16
3.1.4	Second-order transfer function with complex poles	16
3.1.5	Second-order transfer function with multiple poles	16
3.2	Generalized second-order transfer functions	20
3.2.1	Generalized second-order transfer functions	20
3.2.2	Electrochemical examples	20
3.2.3	Canonical form	20
3.2.4	Reduced form	20
3.2.5	Complex poles $\zeta < 1$	20

3.2.6	Multiple poles $\zeta = 1$	23
3.2.7	Real poles $\zeta > 1$	25
4	Appendix: 3D-plot of transfer functions	27
4.1	3D-plot of modulus [3]	27
4.1.1	First order transfer function	27
4.1.2	Second order transfer function	27
	Bibliography	29

Chapter 1

Graphs of transfer functions

1.1 Introduction [1]

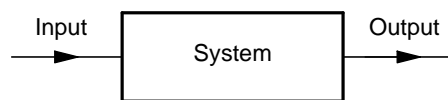


Figure 1.1: Sketch of a scalar system.

- The transfer function, H , of a invariant scalar linear system is given by:

$$H(s) = \frac{\mathcal{L}[\text{Output}]}{\mathcal{L}[\text{Input}]}$$

\mathcal{L} denotes the Laplace transform, s is the Laplace variable with $s = \sigma + i\omega$. For current input and potential output, H is an impedance.

- A transfer function is a complex function $H(s)$ of two real variables σ and ω . It is not possible to plot graph of $H(s)$ in a plane, only 3D-plots are possible [3] (cf. Chap. 4).
- For $s = i\omega$, *i.e.* $\sigma = 0$, corresponding to frequencial analysis, a transfer function is a complex function $H = H(i\omega)$ (or $H(\omega)$) of a real variable ω . It is possible to plot graph of $H = H(\omega)$ in a plane and different types of graph can be used.
- The order of rational fraction transfer function is the degree in s (or $i\omega$) of the transfer function denominator.
 - The relativer order of rational fraction transfer function is the difference between the order of the denominator and the order of the numerator.
 - A proper system is a system where the degree of the denominator is larger or equal to the degree of the numerator.
 - A strictly proper system is a system where the degree of the denominator is larger than the degree of the numerator.

- Poles of transfer function are the roots of the denominator of the transfer function $H(s)$.
 - Dominant poles: poles closest to the imaginary axis
- Zeros of transfer function are the roots of the numerator of the transfer function $H(s)$.

1.2 Nyquist diagram

1.2.1 Nyquist diagram used by electricians

Orthonormal parametric plot

$$x = \operatorname{Re} H = f(\omega), \quad y = \operatorname{Im} H = g(\omega) \quad (1.1)$$

1.2.2 Nyquist diagram used by electrochemists

Orthonormal parametric plot

$$x = \operatorname{Re} H = f(\omega), \quad y = -\operatorname{Im} H = g(\omega) \quad (1.2)$$

1.3 Bode diagram

1.3.1 Bode diagram used by electricians

- Modulus diagram: $20 \log |H|$ vs. $\log \omega$. $|H|$ is the modulus (or magnitude or amplitude) of H with $|H| = \sqrt{(\operatorname{Re} H)^2 + (\operatorname{Im} H)^2}$.
- Phase diagram: ϕ_H vs. $\log \omega$. ϕ_H is the phase of H with $\phi_H = \arctan \frac{\operatorname{Im} H}{\operatorname{Re} H}$

1.3.2 Bode diagram used by electrochemists

$$\log |H| \text{ vs. } \log \omega, \quad \phi_H \text{ vs. } \log \omega \quad (1.3)$$

1.4 Black diagram

1.4.1 Black diagram used by electrician

Parametric plot

$$x = \phi_H = f(\omega), \quad y = 20 \log |H| = g(\omega) \quad (1.4)$$

1.4.2 Black diagram used by electrochemists

Parametric plot

$$x = \phi_H = f(\omega), \quad y = \log |H| = g(\omega) \quad (1.5)$$

1.5 Miscellaneous

- $\operatorname{Re} H$ vs. $\log \omega$, $\operatorname{Im} H$ vs. $\log \omega$
- $\log \operatorname{Re} H$ vs. $\log \omega$, $\log \operatorname{Im} H$ vs. $\log \omega$ [10, 9]
- $\log \operatorname{Im} H$ vs. $\log \operatorname{Re} H$ [6], $\log |\operatorname{Im} H|$ vs. $\log |\operatorname{Re} H|$

Chapter 2

First-order and generalized first-order transfer functions

2.1 First-order transfer function [2, 7]

2.1.1 First-order transfer function

$$H(s) = \frac{K}{1 + \tau s}, \quad H(\omega) = \frac{K}{1 + i\omega\tau}$$

K : static gain, τ : time constant.

2.1.2 Dimensionless first-order transfer function

$$H^*(S) = \frac{H(s)}{K} = \frac{1}{1 + S}, \quad S = \tau s = \Sigma + iu, \quad \Sigma = \tau\sigma, \quad u = \tau\omega$$

One real pole: $S_p = -1$ (Fig. 2.1).

$$H^*(u) = \frac{H(\omega)}{K} = \frac{1}{1 + iu}, \quad u = \tau\omega \quad (2.1)$$

u : reduced (or dimensionless or nondimensional) angular (or radial) frequency

$$\operatorname{Re} H^*(u) = \frac{1}{1 + u^2}, \quad \operatorname{Im} H^*(u) = -\frac{u}{1 + u^2}, \quad \lim_{u \rightarrow 0} \operatorname{Re} H^*(u) = 1$$

Characteristic frequency: $u_c = 1$ (Fig. 2.1).

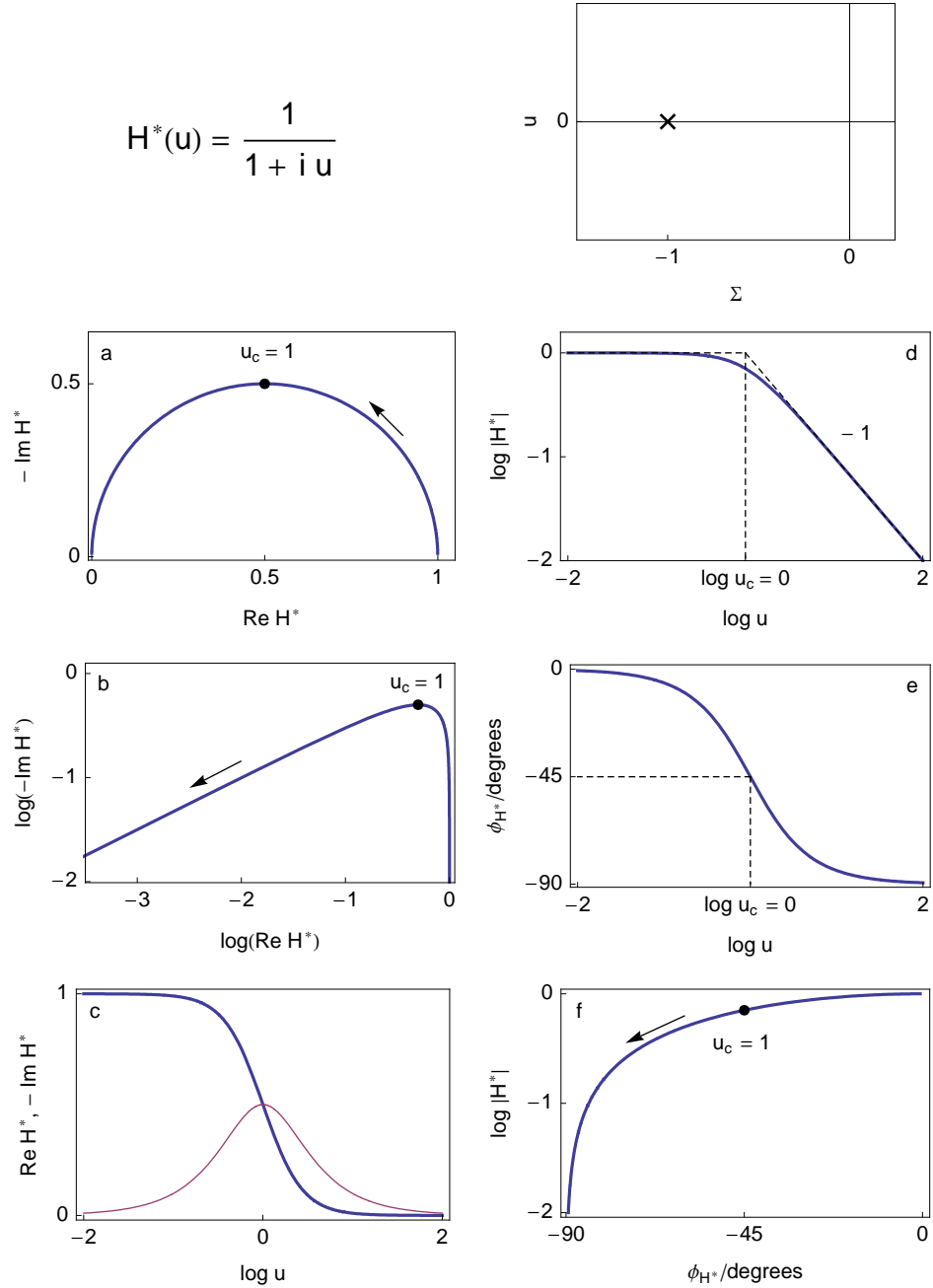


Figure 2.1: Pole-zero map, Nyquist (a), log Nyquist (b) $\text{Re } H^*$ vs. $\log u$ (c, thick line), $-\text{Im } H^*$ vs. $\log u$ (c, thin line), Bode (modulus (d) and phase (e)) and Black diagrams (f) of the first order transfer function $H^*(u) = 1/(1 + i u)$. Arrow always indicates increasing angular frequencies.

2.2 Generalized first-order transfer functions

2.2.1 High-pass first-order transfer function

$$H(s) = \frac{K \tau_N s}{1 + \tau_D s}, \quad H(\omega) = \frac{K \tau_N i \omega}{1 + \tau_D i \omega}$$

2.2.2 Dimensionless high-pass first-order transfer function

$$H^*(S) = \frac{H(s)}{K r_\tau} = \frac{S}{1 + S}, \quad r_\tau = \frac{\tau_N}{\tau_D}, \quad S = \tau_D s = \Sigma + i u, \quad \Sigma = \tau_D \sigma, \quad u = \tau_D \omega$$

One real pole: $S_p = -1$, one zero at the origin: $S_z = 0$ (Fig. 2.2).

$$H^*(u) = \frac{H(\omega)}{r_\tau} = \frac{i u}{1 + i u}, \quad u = \tau_D \omega$$

$$\begin{aligned} \operatorname{Re} H^*(u) &= \frac{u^2}{1 + u^2}, \quad \operatorname{Im} H^*(u) = \frac{u}{1 + u^2} \\ \lim_{u \rightarrow \infty} \operatorname{Re} H^*(u) &= 1 \end{aligned}$$

Characteristic frequency: $u_c = 1$ (Fig. 2.2).

2.2.3 Generalized first-order transfer function

$$H(s) = \frac{K(1 + \tau_N s)}{1 + \tau_D s}, \quad H(\omega) = \frac{K(1 + \tau_N i \omega)}{1 + \tau_D i \omega}$$

2.2.4 Dimensionless generalized first-order transfer function

$$H^*(S) = \frac{H(S)}{K} = \frac{1 + r_\tau S}{1 + S}, \quad r_\tau = \frac{\tau_N}{\tau_D}, \quad S = \tau_D s = \Sigma + i u, \quad \Sigma = \tau_D \sigma, \quad u = \tau_D \omega$$

One real pole: $S_p = -1 = -u_{c1}$, one real zero: $S_z = -1/r_\tau = -u_{c2}$.

$$H^*(u) = \frac{H(u)}{K} = \frac{1 + i r_\tau u}{1 + i u}$$

$$\begin{aligned} \operatorname{Re} H^*(u) &= \frac{1 + r_\tau u^2}{1 + u^2}, \quad \operatorname{Im} H^*(u) = \frac{(-1 + r_\tau) u}{1 + u^2} \\ \lim_{u \rightarrow 0} \operatorname{Re} H^*(u) &= 1, \quad \lim_{u \rightarrow \infty} \operatorname{Re} H^*(u) = r_\tau \end{aligned}$$

Characteristic frequency: $u_{c1} = 1$, $u_{c2} = 1/r_\tau$ ($\phi_{u_{c1}} = \phi_{u_{c2}}$).

$r_\tau < 1 \Rightarrow$ Capacitive behaviour (Fig. 2.3).

$r_\tau > 1 \Rightarrow$ Inductive behaviour (Fig. 2.4).

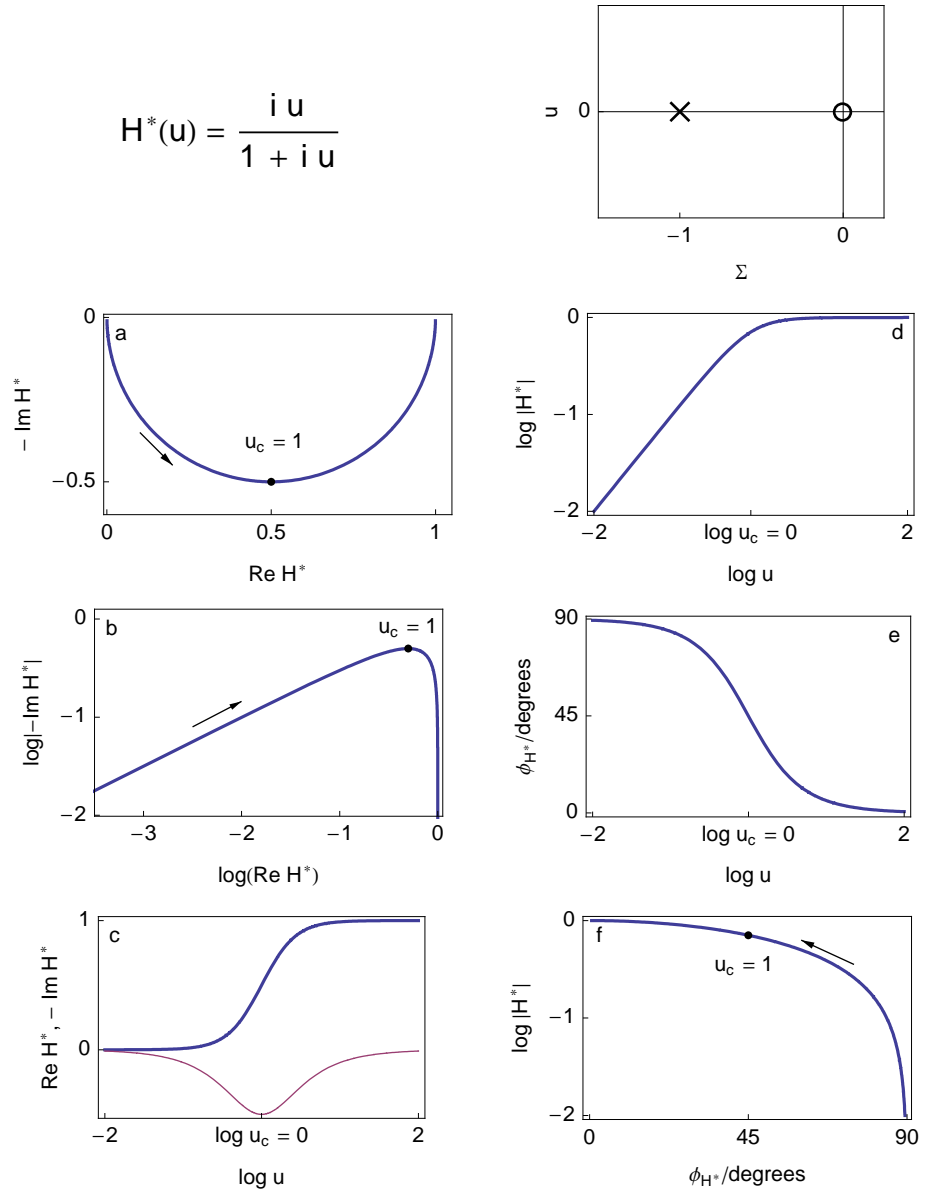


Figure 2.2: Pole-zero map, Nyquist (a), log Nyquist (b) $\text{Re } H^*$ vs. $\log u$ (c, thick line), $-\text{Im } H^*$ vs. $\log u$ (c, thin line), Bode (modulus (c) and phase (d)) and Black diagrams of the high-pass first-order transfer function. Arrow always indicates increasing angular frequencies.

$$H^*(u) = \frac{1 + r_\tau i u}{1 + i u}$$

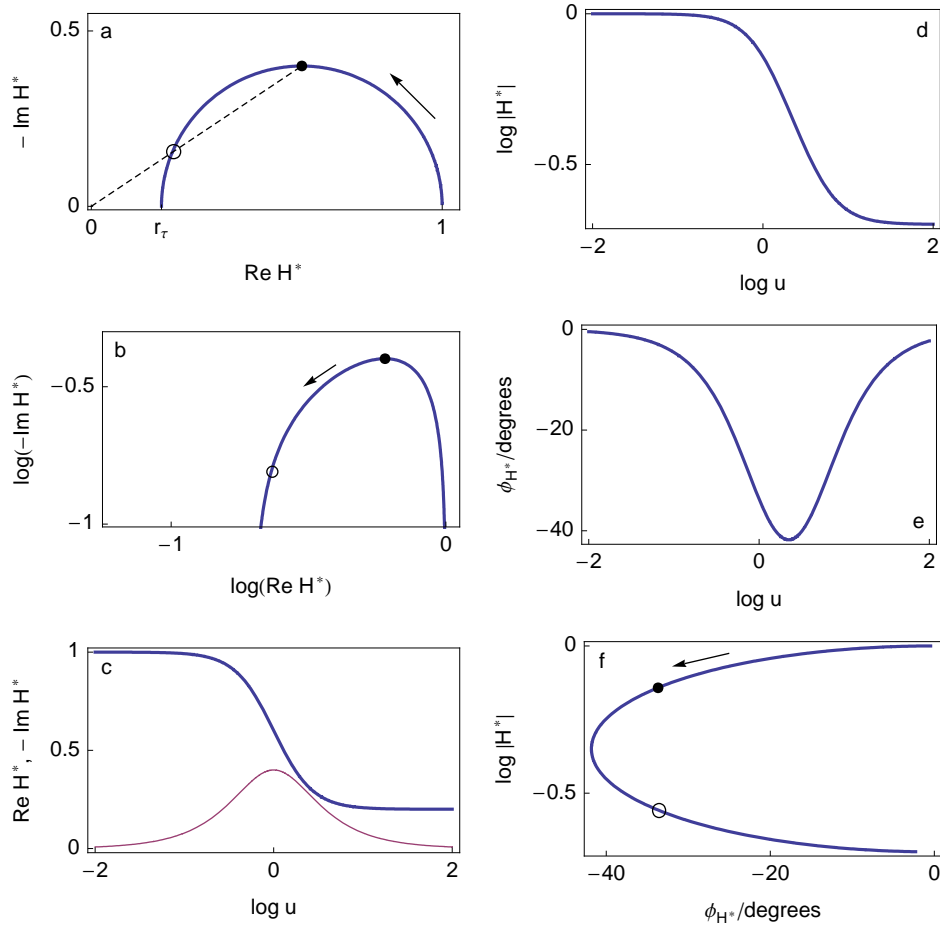
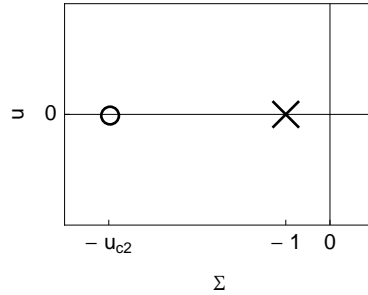


Figure 2.3: Pole-zero map, Nyquist (a), log Nyquist (b) $\text{Re } H^*$ vs. $\log u$ (c, thick line), $-\text{Im } H^*$ vs. $\log u$ (c, thin line), Bode (modulus (c) and phase (d)) and Black diagrams of the generalized first order transfer function. $r_\tau = 0.2$ ($r_\tau < 1$), dot: $u_{c1} = 1$, circle: $u_{c2} = 1/r_\tau$.

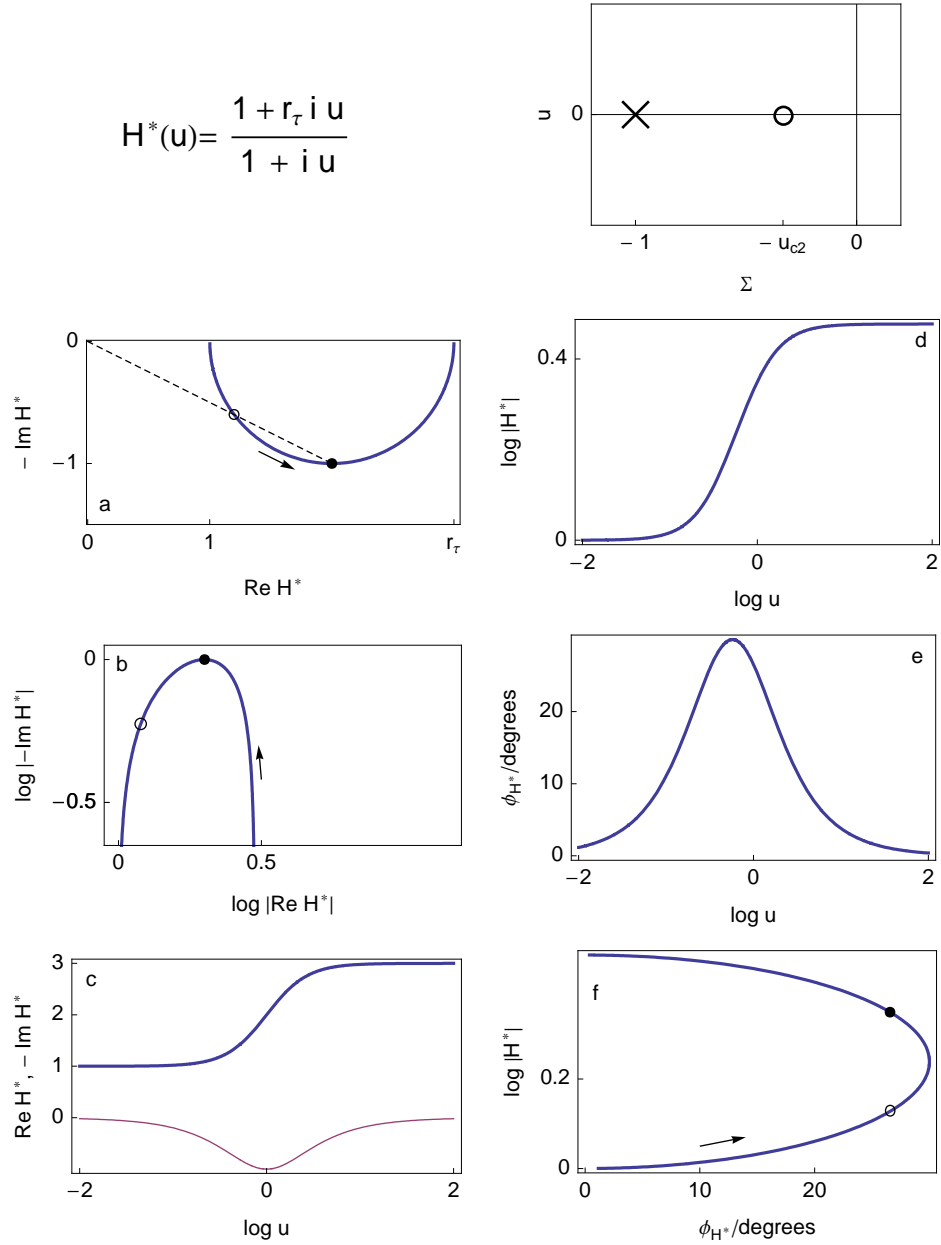


Figure 2.4: Pole-zero map, Nyquist (a), log Nyquist (b) $\text{Re } H^*$ vs. $\log u$ (c, thick line), $-\text{Im } H^*$ vs. $\log u$ (c, thin line), Bode (modulus (c) and phase (d)) and Black diagrams of the generalized first order transfer function. $r_\tau = 3$ ($r_\tau > 1$), dot: $u_{c1} = 1$, circle: $u_{c2} = 1/r_\tau$.

Chapter 3

Second-order and generalized second-order transfer functions

3.1 Introduction

$$H(s) = \frac{K}{1 + a_1 s + a_2 s^2}$$

3.1.1 Canonical form

$$H(s) = \frac{K}{1 + 2\zeta \frac{s}{\omega_n} + \left(\frac{s}{\omega_n}\right)^2}$$

poles:

$$s_{p1} = -\zeta\omega_n - \sqrt{(\zeta^2 - 1)\omega_n^2}, \quad s_{p2} = -\zeta\omega_n + \sqrt{(\zeta^2 - 1)\omega_n^2}$$

- $\zeta > 1$, two real poles
- $\zeta = 1$ multiple pole
- $\zeta < 1$ complex poles

3.1.2 Reduced form

$$H^*(S) = \frac{H(s)}{K} = \frac{1}{1 + 2\zeta S + S^2}, \quad S = \frac{s}{\omega_n} = \frac{\sigma + i\omega}{\omega_n} = \Sigma + i u, \quad \Sigma = \frac{\sigma}{\omega_n}, \quad u = \frac{\omega}{\omega_n}$$

poles:

$$S_{p1} = -\zeta - \sqrt{\zeta^2 - 1}, \quad S_{p2} = -\zeta + \sqrt{\zeta^2 - 1}$$

3.1.3 Second-order transfer function with real poles

$$H(s) = \frac{K}{(1 + \tau_1 s)(1 + \tau_2 s)}, \quad H(\omega) = \frac{K}{(1 + \tau_1 i\omega)(1 + \tau_2 i\omega)}$$

$$H^*(S) = \frac{H(s)}{K} = \frac{1}{(1 + S)(1 + r_\tau S)}, \quad S = \tau_1 s = \Sigma + iu, \quad \Sigma = \tau_1 \sigma, \quad u = \tau_1 \omega, \quad r_\tau = \frac{\tau_2}{\tau_1}$$

Two real poles: $S_{p1} = -1 = -u_{c1}$, $S_{p2} = -1/r_\tau = -u_{c2}$ (Fig. 3.1).

$$H^*(u) = \frac{1}{(1 + iu)(1 + r_\tau iu)}$$

$$\text{Re } H^*(u) = \frac{1 - u^2 r_\tau}{(1 + u^2)(1 + u^2 r_\tau^2)}, \quad \text{Im } H^*(u) = -\frac{u(1 + r_\tau)}{(1 + u^2)(1 + u^2 r_\tau^2)}$$

3.1.4 Second-order transfer function with complex poles

$$H^*(S) = \frac{1}{1 + 2\zeta S + S^2}, \quad \zeta < 1$$

Two complex poles (Fig. 3.2) :

$$S_{p1} = -\zeta - \sqrt{\zeta^2 - 1} = -\zeta - i\sqrt{1 - \zeta^2}, \quad S_{p2} = -\zeta + \sqrt{\zeta^2 - 1} = -\zeta + i\sqrt{1 - \zeta^2}$$

$$H^*(u) = \frac{1}{1 + 2\zeta iu + (iu)^2}, \quad \zeta < 1$$

$$\text{Re } H^*(u) = \frac{1 - u^2}{u^4 + (4\zeta^2 - 2)u^2 + 1}, \quad \text{Im } H^*(u) = -\frac{2u\zeta}{u^4 + (4\zeta^2 - 2)u^2 + 1}$$

3.1.5 Second-order transfer function with multiple poles

$$H^*(S) = \frac{1}{1 + 2\zeta S + S^2}, \quad \zeta = 1 \Rightarrow H^*(S) = \frac{1}{(1 + S)^2}$$

One multiple pole: $S_p = -1 \Rightarrow u_c = 1$ (Fig. 3.3).

$$H^*(u) = \frac{1}{(1 + iu)^2}$$

$$\text{Re } H^*(u) = \frac{1 - u^2}{(u^2 + 1)^2}, \quad \text{Im } H^*(u) = -\frac{2u}{(u^2 + 1)^2}$$

$$\frac{d\text{Im}(u)}{du} = 0 \Rightarrow \omega = \frac{1}{\sqrt{3}}, \quad H^*(u) = \frac{3}{8}(1 - i\sqrt{3})$$

$$\frac{d\text{Re}(u)}{du} = 0 \Rightarrow \omega = \sqrt{3}, \quad H^*(u) = -\frac{1}{8}(1 + i\sqrt{3})$$

$$H^*(u) = \frac{1}{(1 + iu)(1 + r_\tau iu)}$$

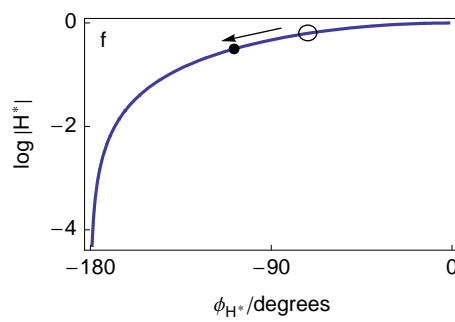
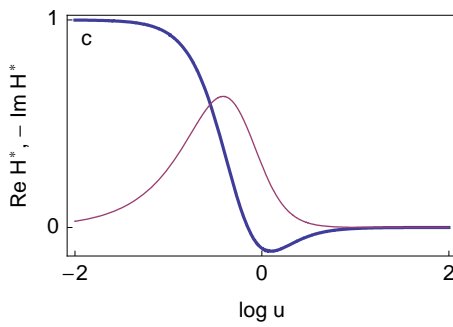
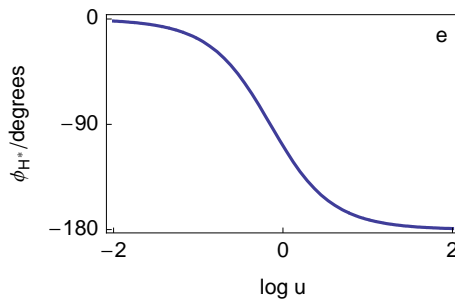
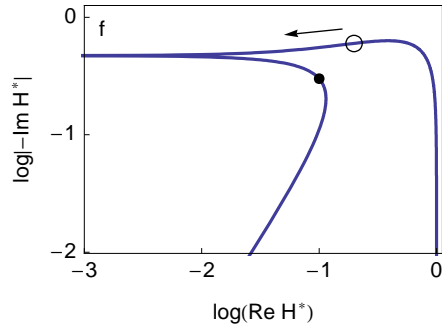
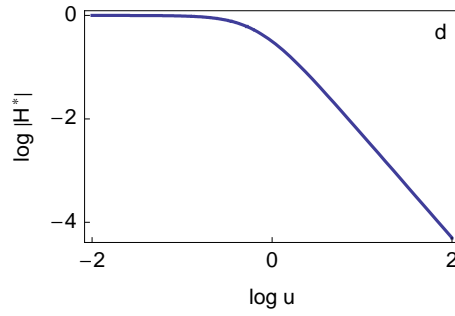
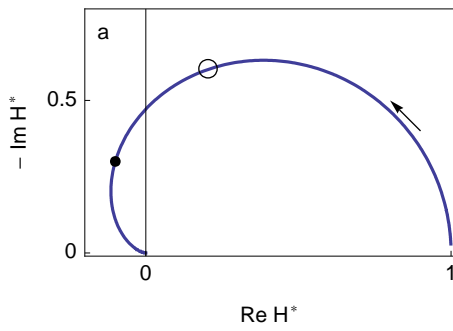
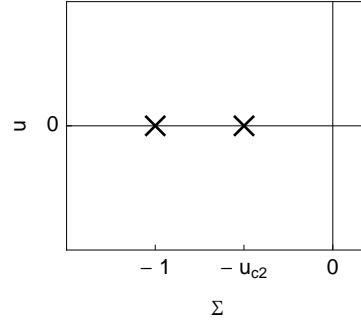


Figure 3.1: Pole-zero map, Nyquist (a), log Nyquist (b) $\text{Re } H^*$ vs. $\log u$ (c, thick line), $-\text{Im } H^*$ vs. $\log u$ (c, thin line), Bode (modulus (c) and phase (d)) and Black diagrams of the reduced second order transfer function with real poles $H^* = 1/((1 + iu)(1 + r_\tau iu))$. $r_\tau = 2$ ($r_\tau > 1$), dot: $u_{c1} = 1$, circle: $u_{c2} = 1/r_\tau$.

$$H^*(u) = \frac{1}{1 + 2\zeta i u + (i u)^2}$$

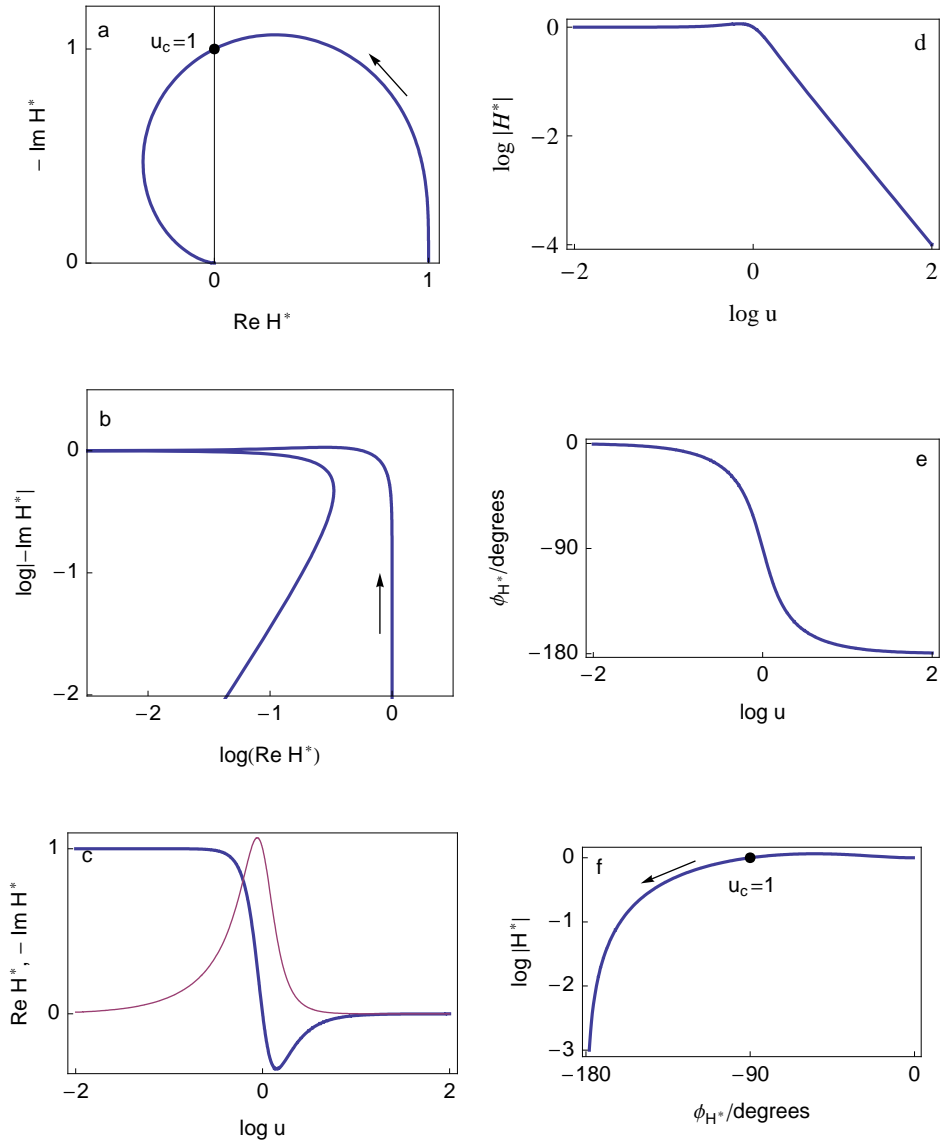
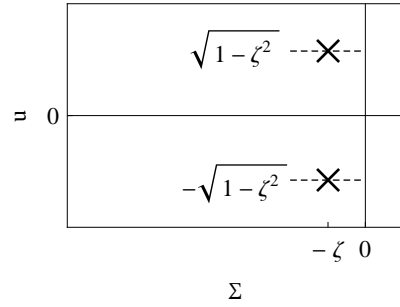


Figure 3.2: Pole-zero map, Nyquist (a), log Nyquist (b) $\text{Re } H^*$ vs. $\log u$ (c, thick line), $-\text{Im } H^*$ vs. $\log u$ (c, thin line), Bode (modulus (d) and phase (e)) and Black diagrams of the reduced second order transfer function with complex poles $H^*(u) = 1/(1 + 2\zeta i u + (i u)^2)$, $\zeta = 0.5$.

$$H^*(u) = \frac{1}{(1 + i u)^2}$$

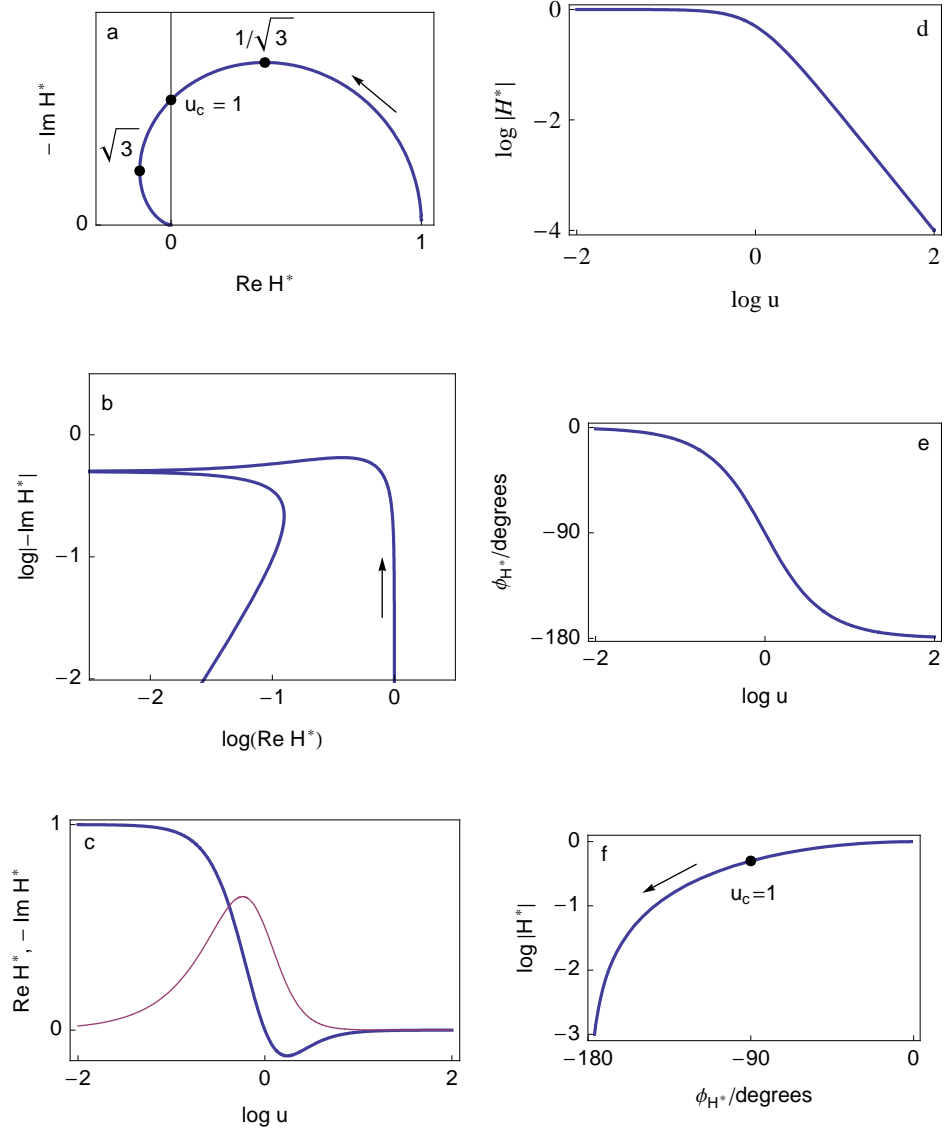
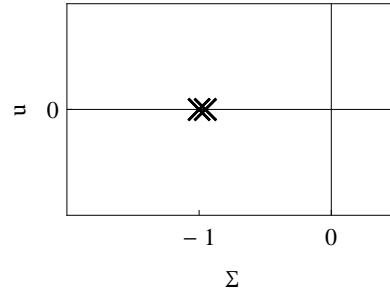


Figure 3.3: Pole-zero map, Nyquist (a), log Nyquist (b) $\text{Re } H^*$ vs. $\log u$ (c, thick line), $-\text{Im } H^*$ vs. $\log u$ (c, thin line), Bode (modulus (c) and phase (d)) and Black diagrams of the reduced second order transfer function with multiple poles $H^*(u) = 1/(1 + i u)^2$.

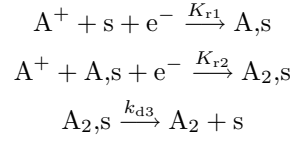
3.2 Generalized second-order transfer functions

3.2.1 Generalized second-order transfer functions

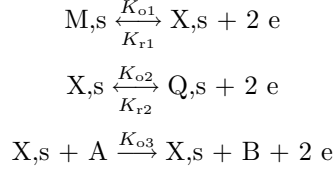
$$H(s) = \frac{K(1 + b_1 s)}{1 + a_1 s + a_2 s^2}$$

3.2.2 Electrochemical examples

Volmer-Heyrovský reaction with chemical desorption [8, 4, 5]



Schuhmann dissolution-passivation reaction # 1 [11]



3.2.3 Canonical form

$$H(s) = \frac{K(1 + b_1 s)}{1 + 2\zeta \frac{s}{\omega_n} + \left(\frac{s}{\omega_n}\right)^2}$$

poles:

$$\begin{aligned} s_{p1} &= -\zeta\omega_n - \sqrt{(\zeta^2 - 1)\omega_n^2}, \quad s_{p2} = -\zeta\omega_n + \sqrt{(\zeta^2 - 1)\omega_n^2} \\ \zeta > 1, & \text{ two real poles, } \zeta = 1 \text{ multiple pole, } \zeta < 1 \text{ complex poles (cf. 3.1.1).} \end{aligned}$$

3.2.4 Reduced form

$$H^*(S) = \frac{H(s)}{K} = \frac{1 + TS}{1 + 2\zeta S + S^2}, \quad S = \frac{s}{\omega_n} = \frac{\sigma + i\omega}{\omega_n} = \Sigma + iu, \quad \Sigma = \frac{\sigma}{\omega_n}, \quad u = \frac{\omega}{\omega_n}$$

poles: $S_{p1} = -\zeta - \sqrt{\zeta^2 - 1}$, $S_{p2} = -\zeta + \sqrt{\zeta^2 - 1}$, zero: $S_z = -1/T$.

$$\operatorname{Re} H^*(u) = \frac{(2T\zeta - 1)u^2 + 1}{u^4 + (4\zeta^2 - 2)u^2 + 1}, \quad \operatorname{Im} H^*(u) = \frac{u(-Tu^2 + T - 2\zeta)}{u^4 + (4\zeta^2 - 2)u^2 + 1}$$

$\Rightarrow \operatorname{Im} H^*(u) > 0$ (inductif behaviour) for $0 < u < \sqrt{T - 2\zeta}/\sqrt{T}$ if $T > 2\zeta$.

3.2.5 Complex poles $\zeta < 1$

- $T > 1$: Fig. 3.4,
- $T = 1$: Fig. 3.5,
- $T < 1$: Figs. 3.6 and 3.7.

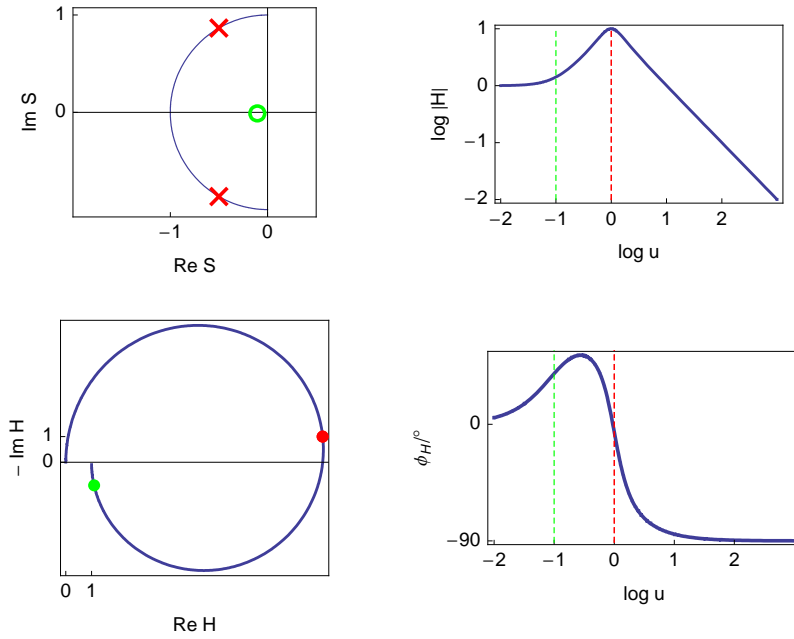


Figure 3.4: Pole-zero map, Nyquist, Bode (modulus and phase) of the reduced generalized second-order transfer function with complex poles $H^*(u) = (1 + T i u)/(1 + 2 \zeta i u + (i u)^2)$. $\zeta = 0.5$, $T = 10$.

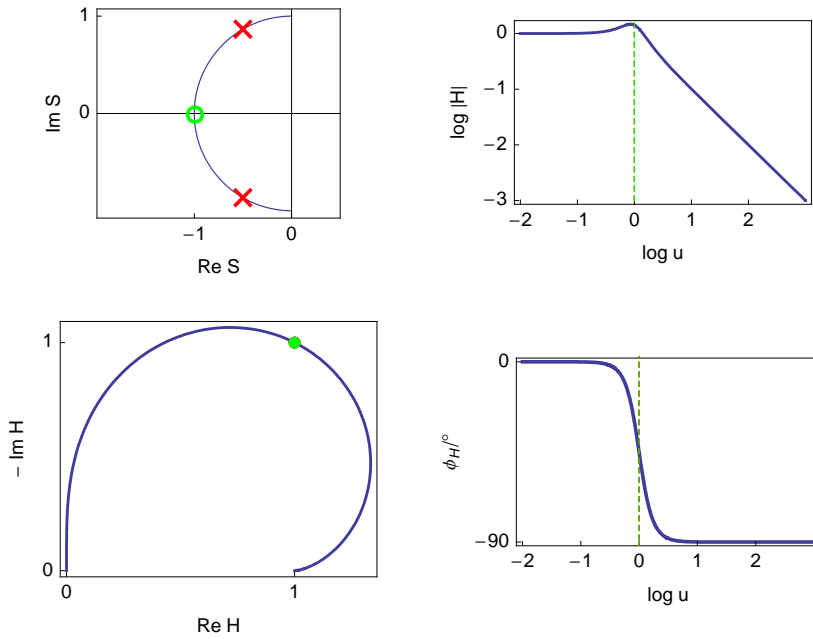


Figure 3.5: Pole-zero map, Nyquist, Bode (modulus and phase) of the reduced generalized second-order transfer function with complex poles $H^*(u) = (1 + T i u)/(1 + 2 \zeta i u + (i u)^2)$. $\zeta = 0.5$, $T = 1$.

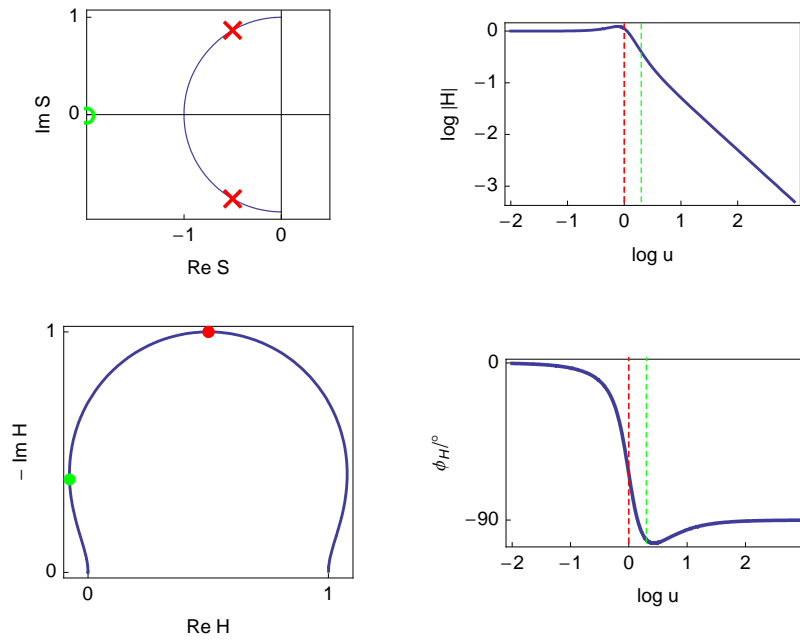


Figure 3.6: Pole-zero map, Nyquist, Bode (modulus and phase) of the reduced generalized second-order transfer function with complex poles $H^*(u) = (1 + T i u)/(1 + 2 \zeta i u + (i u)^2)$. $\zeta = 0.5$, $T = 0.5$.

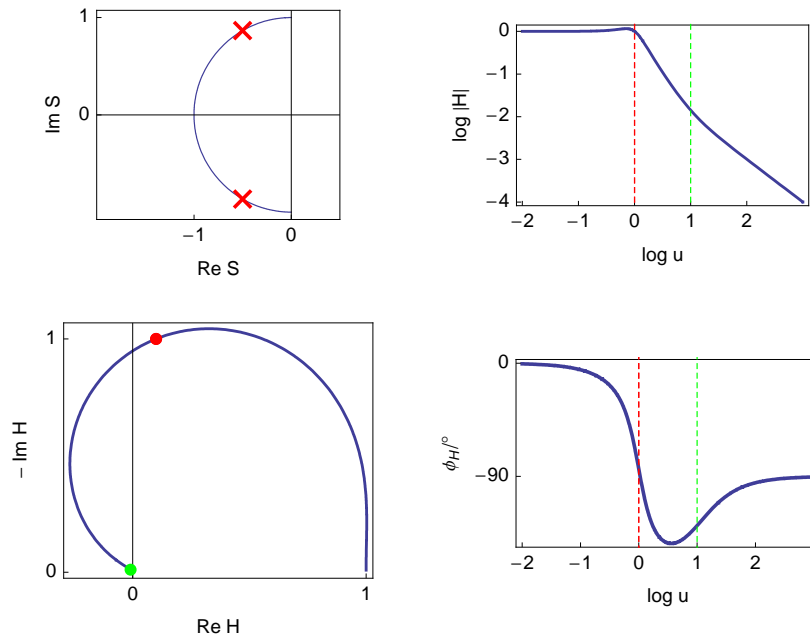


Figure 3.7: Pole-zero map, Nyquist, Bode (modulus and phase) of the reduced generalized second-order transfer function with complex poles $H^*(u) = (1 + T i u)/(1 + 2 \zeta i u + (i u)^2)$. $\zeta = 0.5$, $T = 0.1$. Zero not shown in the pole-zero map.

3.2.6 Multiple poles $\zeta = 1$

- $T > 1$: Fig. 3.8,
- $T = 1$: Fig. 3.9,
- $T < 1$: Fig. 3.10.

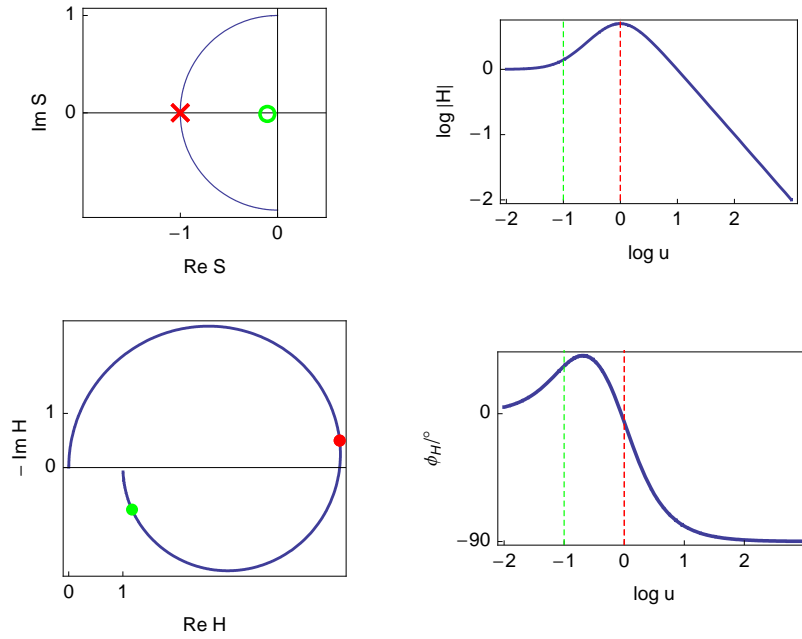


Figure 3.8: Pole-zero map, Nyquist, Bode (modulus and phase) of the reduced generalized second-order transfer function with multiple poles $H^*(u) = (1 + T i u)/(1 + 2 \zeta i u + (i u)^2)$. $\zeta = 1$, $T = 10$.

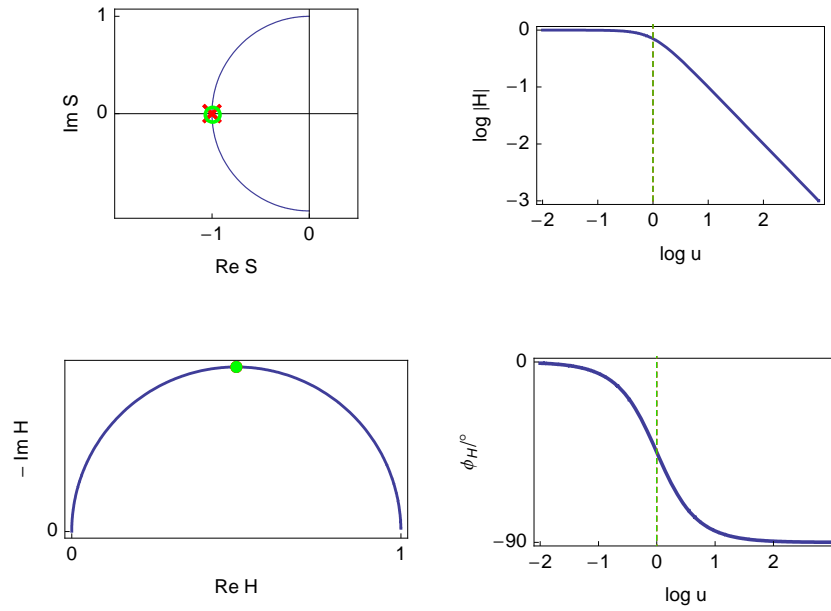


Figure 3.9: Pole-zero map, Nyquist, Bode (modulus and phase) of the reduced generalized second-order transfer function with multiple poles $H^*(u) = (1 + T i u)/(1 + 2 \zeta i u + (i u)^2)$. $\zeta = 1$, $T = 1$.

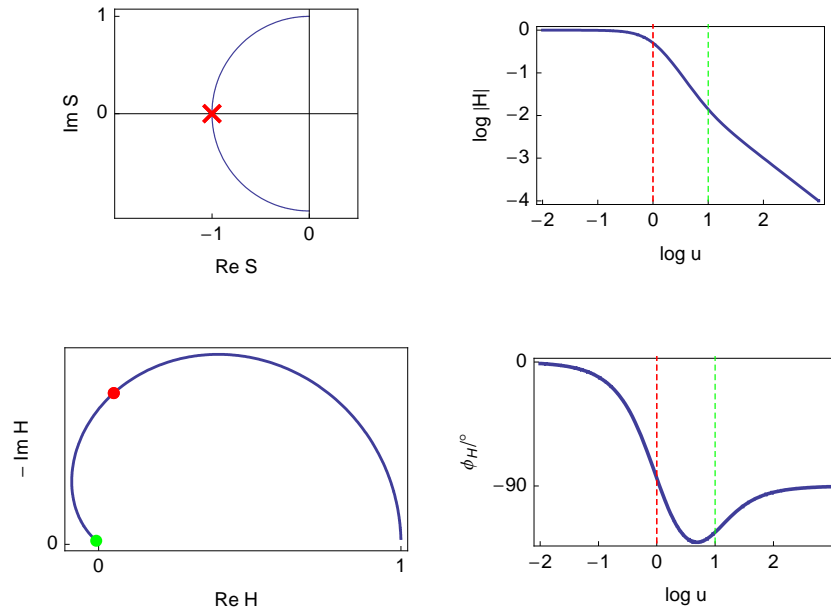


Figure 3.10: Pole-zero map, Nyquist, Bode (modulus and phase) of the reduced generalized second-order transfer function with multiple poles $H^*(u) = (1 + T i u)/(1 + 2 \zeta i u + (i u)^2)$. $\zeta = 1$, $T = 1$. Zero not shown in the pole-zero map

3.2.7 Real poles $\zeta > 1$

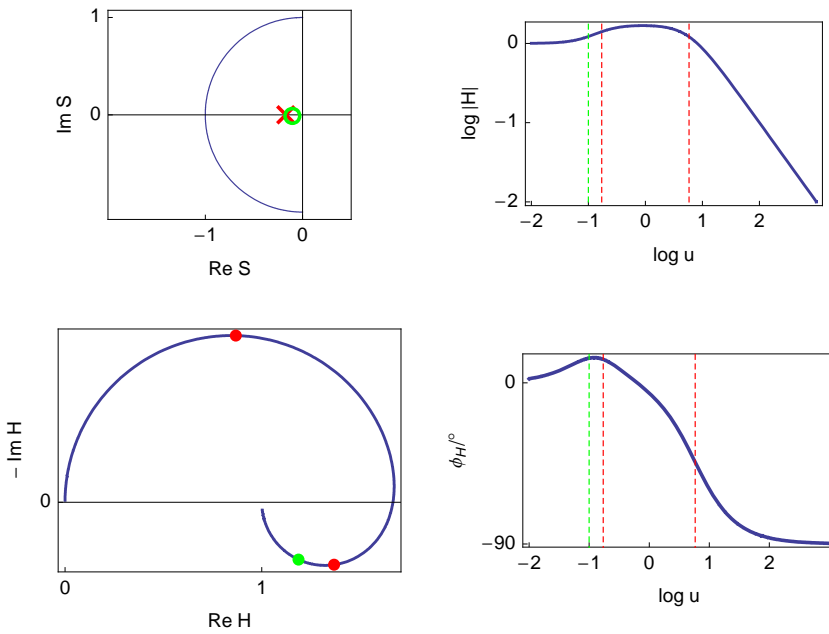
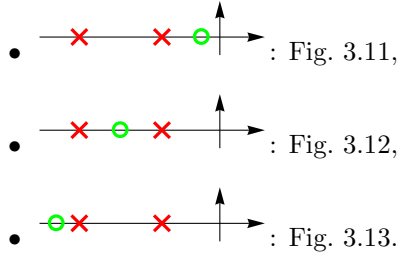


Figure 3.11: Pole-zero map, Nyquist, Bode (modulus and phase) of the reduced generalized second-order transfer function with real poles $H^*(u) = (1 + T i u)/(1 + 2 \zeta i u + (i u)^2)$. $\zeta = 3, T = 10$.

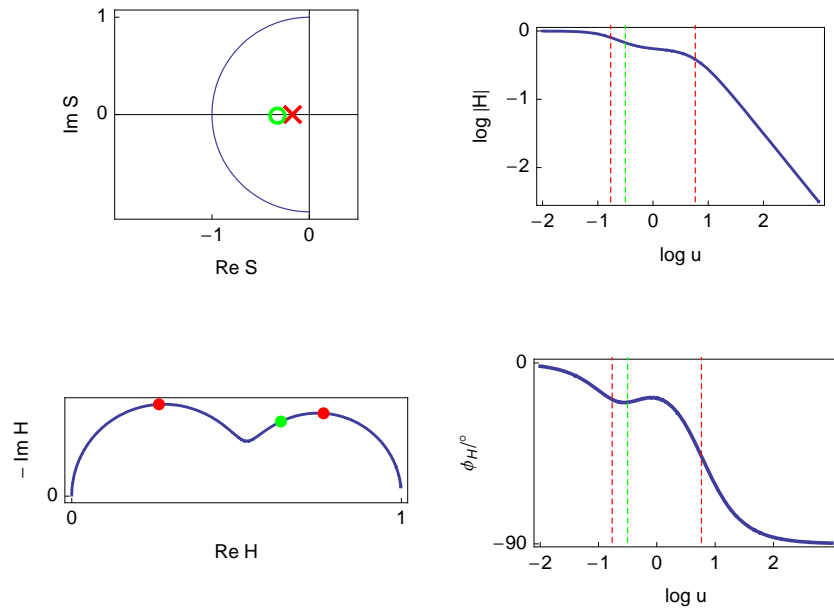


Figure 3.12: Pole-zero map, Nyquist, Bode (modulus and phase) of the reduced generalized second-order transfer function with real poles $H^*(u) = (1 + T i u)/(1 + 2 \zeta i u + (i u)^2)$. $\zeta = 3$, $T = 3.16$. One pole not shown in the pole-zero map.

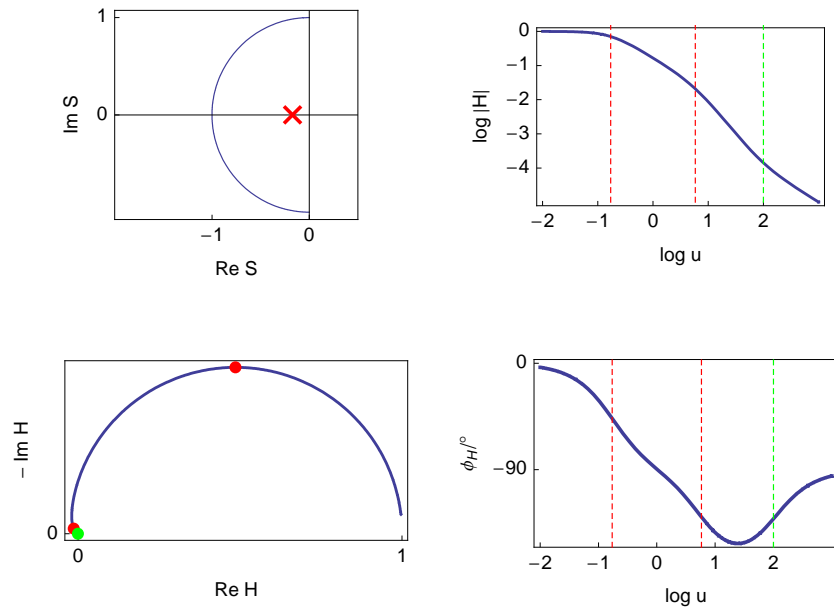


Figure 3.13: Pole-zero map, Nyquist, Bode (modulus and phase) of the reduced generalized second-order transfer function with real poles $H^*(u) = (1 + T i u)/(1 + 2 \zeta i u + (i u)^2)$. $\zeta = 3$, $T = 10^{-2}$. Zero and one pole not shown in the pole-zero map.

Chapter 4

Appendix: 3D-plot of transfer functions

4.1 3D-plot of modulus [3]

4.1.1 First order transfer function

$$H^*(S) = \frac{1}{1+S}, \quad S = \Sigma + iu$$

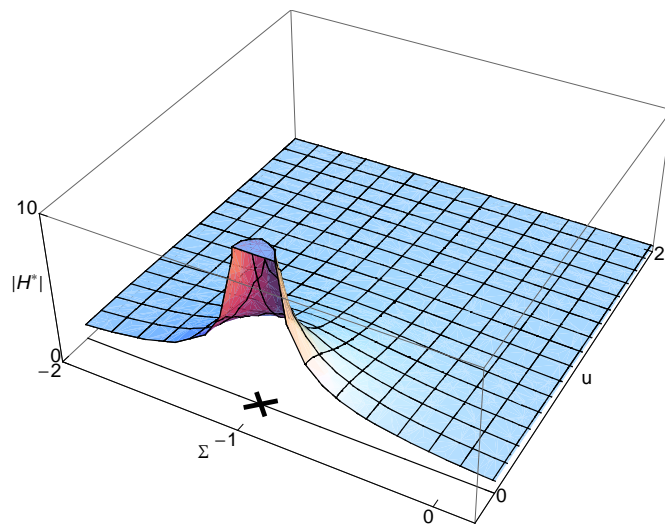


Figure 4.1: 3D-plot of the modulus of first order transfer function.

4.1.2 Second order transfer function

Complex poles

$$H^*(S) = \frac{1}{1 + 2\zeta S + S^2}, \quad S = \Sigma + iu, \quad \zeta < 1$$

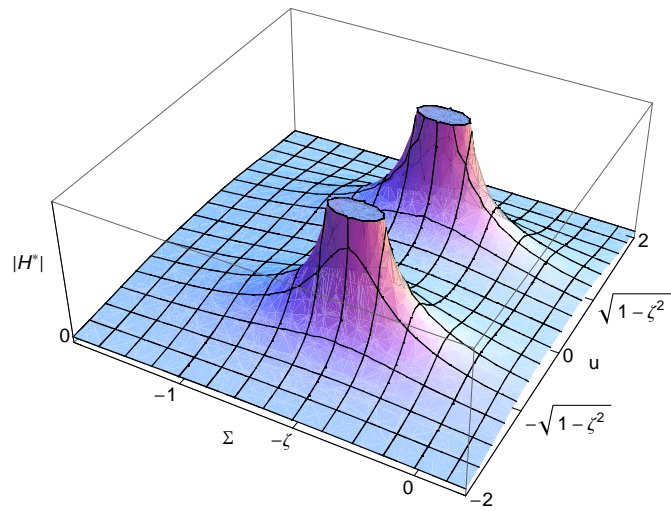


Figure 4.2: 3D-plot of the modulus of second order transfer function. Complex poles, $\zeta = 0.5$

Real poles

$$H^*(S) = \frac{1}{(1+S)(1+r_\tau S)}, S = \Sigma + iu$$

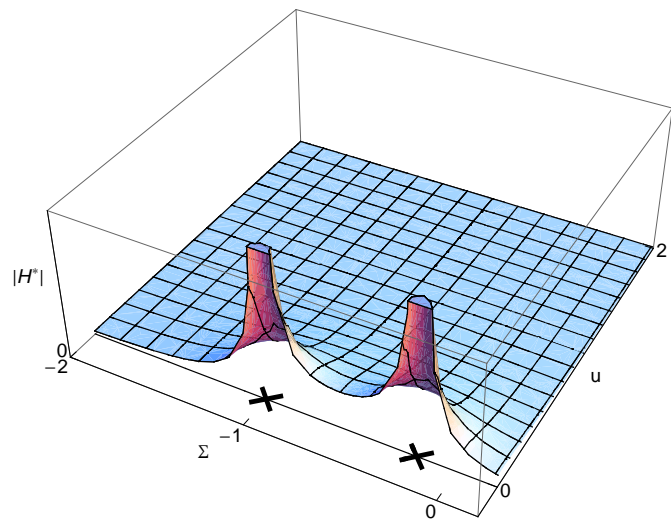


Figure 4.3: 3D-plot of the modulus of second order transfer function. Real poles, $r_\tau = 5$

Bibliography

- [1] Control systems/system metrics. [http://en.wikibooks.org/wiki/Control Systems](http://en.wikibooks.org/wiki/Control_Systems).
- [2] DE LARMINAT, P., AND TOMAS, Y. *Automatique des systèmes linéaire. I. Signaux et systèmes*. Flammarion, Paris, 1975.
- [3] DIARD, J.-P., LEGORREC, B., AND MONTELLA, C. Il n'y a pas que $j\omega$. In *Proceeding of the 7th Forum sur les Impédances Electrochimiques* (Montrouge, 1993), C. Gabrielli, Ed., pp. 133–138. <http://www.Electrochimie.org>.
- [4] DIARD, J.-P., LEGORREC, B., MONTELLA, C., AND MONTERO-OCAMPO, C. Second order electrochemical impedances and electrical resonance phenomenon. *Electrochim. Acta* 37 (1992), 177–179.
- [5] DIARD, J.-P., LEGORREC, B., MONTELLA, C., AND MONTERO-OCAMPO, C. Calculation, simulation and interpretation of electrochemical impedance diagrams. Part IV. Second-order electrochemical impedances. *J. Electroanal. Chem.* 352 (1993), 1–15.
- [6] FOURNIER, J., WRONA, P. K., LASIA, A., LACASSE, R., LALANCETTE, J.-M., MENARD, H., AND BROSSARD, L. *J. Electrochem. Soc.* 139 (1992), 2372.
- [7] GILLE, J.-C., DECAULNE, P., AND PÉLEGRIN, M. *Dynamique de la commande linéaire*. Dunod, Paris, 1991.
- [8] MONTERO-OCAMPO, C. *Impédances électrochimiques du second ordre. Exemple du mécanisme de Volmer-Heyrovský avec désorption chimique*. PhD thesis, Institut National Polytechnique de Grenoble, Grenoble, 1988.
- [9] ORAZEM, M. E., PÉBÈRE, N., AND TRIBOLLET, B. *J. Electrochem. Soc.* 153 (2006), B129.
- [10] RODRIGUEZ-PRESA, M. J., TUCCERI, R. I., FLORIT, M. I., AND POSADAS, D. Constant phase element behavior in the poly(*o*-toluidine) impedance response. *J. Electroanal. Chem.* 502 (2001), 82–90.
- [11] SCHUHMAN, D. Étude phénoménologique à l'aide de schémas réactionnels des impédances faradiques contenant des résistances négatives et des inductances. *J. Electroanal. Chem.* 17 (1968), 45–59.